

# Geometric Scaling Effects in Electrical Field Flow Fractionation. 2. Experimental Results

Bruce K. Gale,\* Karin D. Caldwell,<sup>†</sup> and A. Bruno Frazier<sup>‡</sup>

Department of Mechanical Engineering, University of Utah, 50 South Central Campus Drive, Salt Lake City, Utah 84112

**Geometric scaling of microelectrical field flow fractionation ( $\mu$ -EFFF) systems is investigated experimentally and compared to theory and to macroscale EFFF systems. Experimental results are presented to demonstrate that the miniaturized system operates according to the scaling theory associated with the system. Demonstrated improvements in the channels include increased retention and resolution and decreased peak broadening, electrical time constants, relaxation time, power consumption, and sample size. Additionally, scaling effects related to the compression of separation zones in the miniaturized EFFF systems are discussed.**

A significant research effort has been made over the past decade to explore the technical challenges associated with the miniaturization of biochemical analytical tools for a wide variety of chemical, biological, and pharmaceutical applications.<sup>1</sup> These miniaturized systems integrate sample handling, analysis, detection, and signal processing as well as other pertinent processes.<sup>2</sup> One class of analytical tools that has been demonstrated as a solution to the front end sample processing for many analysis operations (i.e., sample purification, concentration) as well as for a primary separation tool is the miniaturized field flow fractionation (FFF) systems. Researchers have demonstrated several subtypes of miniaturized FFF systems including electrical,<sup>3–5</sup> thermal,<sup>6</sup> and dielectrophoretic<sup>7</sup> FFF systems. The early studies demonstrated the ability to construct miniaturized systems for these well-known FFF subtypes and explored the basic performance characteristics of these miniaturized systems. Recently, our group published a theoretical study on the geometrical scaling effects associated with electrical field flow fractionation (EFFF) systems.<sup>8</sup>

The theoretical study and other papers on microscale FFF<sup>9</sup> predict a significant number of important advantages related to miniaturization of the systems. The first publication regarding characterization of modern EFFF systems appeared in 1993 and addressed the basic operation of the system and demonstrated that retention of polystyrene particles occurred in a manner consistent with theory.<sup>10</sup> The paper addressed the steric transition point, the effects of carrier conductivity, steric mode separations, the effects of relaxation time, and the effects of protein adsorption on polymer particles. Later publications addressed system characterization issues related to the internal electric field<sup>11</sup> and the effect of sample conductivity.<sup>12</sup> Most other papers related to EFFF have specifically addressed applications of the system and did not attempt to discuss system characterization.<sup>13–18</sup> Thus, there is little precedent on how to address instrument characterization issues. Additionally, system characterization issues such as plate heights, resolution, time constants, and channel height effects have only been lightly covered. Significantly, several investigators have recognized that the electrical current in the channel is a better measure of the effective field in the channel than is the applied voltage, but to date, few of the system parameters have been related to the current and no method has been suggested for comparison of systems with different operational parameters or channel geometries. In the early studies on miniaturized EFFF systems, operation of the system was clearly demonstrated, but the utility of the system compared to macroscale systems was not well defined. Thus, there is a significant need for development of methods comparing EFFF instrument configurations, especially as they relate to the channel geometry, if EFFF instrumentation systems are to be improved. Specifically, comparisons between the microscale and macroscale systems need to be made to determine the optimal system characteristics for a given separation or analysis. These issues will provide the basis for discussion in this paper.<sup>8</sup>

\* Corresponding author. Phone: (801) 585–5944. Fax: (801) 585–9826. E-mail: gale@mech.utah.edu.

<sup>†</sup> Present address: Center for Surface Biotechnology, Department of Chemistry, Uppsala University, Sweden.

<sup>‡</sup> Present address: School of Electrical and Computer Engineering, Georgia Institute of Technology, Atlanta, GA 30332.

- (1) *Micro Total Analysis Systems 2000*; Van Den Berg, A., Bergveld, P., Eds.; Kluwer Academic Publishers: Dordrecht, The Netherlands, 2000.
- (2) Van Den Berg, A.; Lammerink, T. S. J. In *Microsystem Technology in Chemistry and Life Sciences*; Manz, A., Becker, H., Eds.; Springer-Verlag: Berlin, 1999; pp 21–50.
- (3) Gale, B. K.; Frazier, A. B.; Caldwell, K. D. *Proc. MEMS '97*, **1997**, 119–124.
- (4) Gale, B. K.; Caldwell, K. D.; Frazier, A. B. *IEEE Trans. Biomed. Eng.* **1998**, *45*, 1459–1469.
- (5) Gale, B. K.; Caldwell, K. D.; Frazier, A. B. *Proc. IEEE 1998 Solid-State Sensor and Actuator Workshop* **1998**, 342–345.
- (6) Edwards, T. L.; Gale, B. K.; Frazier, A. B. *Proc. Transducers '99*, **1999**, 742–745.
- (7) Yang, J.; Huang, Y.; Wang, X.-B.; Becker, F. F.; Gascoyne, P. R. C. *Anal. Chem.* **1999**, *71*, 911–918.

- (8) Gale, B. K.; Caldwell, K. D.; Frazier, A. B. *Anal. Chem.* **2001**, *73*, 2345–2352.
- (9) Giddings, J. C. *J. Microcolumn Sep.* **1993**, *5*, 497–503.
- (10) Caldwell, K. D.; Gao, Y. S. *Anal. Chem.* **1993**, *65*, 1764–1772.
- (11) Palkar, S. A.; Schure, M. R. *Anal. Chem.* **1997**, *69*, 3223–3229.
- (12) Palkar, S. A.; Schure, M. R. *Anal. Chem.* **1997**, *69*, 3230–3238.
- (13) Mori, R.; Nakagama, T.; Hobo, T. *Kuromatogurafi* **1994**, *15*, 270–271.
- (14) Schimpf, M. E.; Russell, D. D.; Lewis, J. K. *J. Liq. Chromatogr.* **1994**, *17*, 3221–3238.
- (15) Palkar, S. A.; Murphy, R. E.; Schure, M. R. *Polym. Mater. Sci. Eng.* **1996**, *75*, 6–7.
- (16) Schimpf, M. E.; Caldwell, K. D. *Am. Lab.* **1995**, *27*, 64–68.
- (17) Dunkel, M.; Tri, N.; Beckett, R.; Caldwell, K. D. *J. Microcolumn Sep.* **1997**, *9*, 177–183.
- (18) Nakagama, T.; Hobo, T. *Kuromatogurafi* **1993**, *14*, 114–117.

## METHODS

The methods for characterization of some EFFF system properties have already been proposed by other investigators. For the instances in which a method and results have already been published, an effort will be made to duplicate the experiments using the  $\mu$ -EFFF system, so that the results will be comparable. System properties that are addressed in this section include electrical time constants, current–voltage relationships, current flow rate relationships, plate heights, retention, resolution, steric transition points, relaxation times, and effective field strengths.

The basics regarding  $\mu$ -EFFF system components and setup have been published previously.<sup>4</sup> The specific fractionators used in this work include a macroscale graphite electrode system with a channel 64 cm long, 2 cm in breadth, and 176  $\mu\text{m}$  in height. The microscale systems used for the majority of this work include a channel with gold electrodes that measured 5.4 cm in length, 6 mm in width, and 28  $\mu\text{m}$  in height and a channel with platinum electrodes that measured 5.4 cm in length, 2 mm in width, and 28.5  $\mu\text{m}$  in height. Several system components and operational parameters were common to all of the experiments performed. A Hewlett-Packard 6128C dc power supply was connected to the channel electrodes. Sample injection was made using either a 0.5- or 10- $\mu\text{L}$  Hamilton microsyringe with a normal injection volume of 0.1  $\mu\text{L}$ . Fresh deionized water with a highly controlled resistivity was used as the carrier for all experiments in the microscale systems. The polystyrene latex particles used in these experiments were of an array of sizes from 19 nm to 1  $\mu\text{m}$  and were either from Bangs Laboratories or Interfacial Dynamics Corp. The particles used were identical to those used in earlier studies,<sup>17</sup> so data obtained in those studies were used for estimating the electrophoretic mobility of the particles. The off-chip detector used in the experiments was a Linear UV-106 extinction detector monitoring extinction at 254 nm. The on-chip detector<sup>19,20</sup> consisted of a pair of electrical wires at the end of the EFFF channel through which the impedance across the channel was monitored. The detectors were connected to a recording device (either a PC with LabView software or a strip chart recorder), which collected the data output from the detector as well as the measured current and the applied voltage.

The basic electrical properties of EFFF systems include the current–voltage relationship for variations in flow rate, the time constant for system equilibration, and the effective field in the channel. The relationship between voltage and current was plotted after a 2-min settling time for a range of voltages and flow rates.<sup>21</sup> The electrical time constant,  $\tau$ , was estimated using a step response test.<sup>22</sup> Last, the effective voltage in the channel,  $V_{\text{eff}}$ , was calculated from retention data using the equation

$$V_{\text{eff}} = 6D/\mu R \quad (1)$$

where  $D$  is the particles' diffusion constant,  $\mu$  is their electrophoretic mobility, and  $R$  is the experimentally measured retention

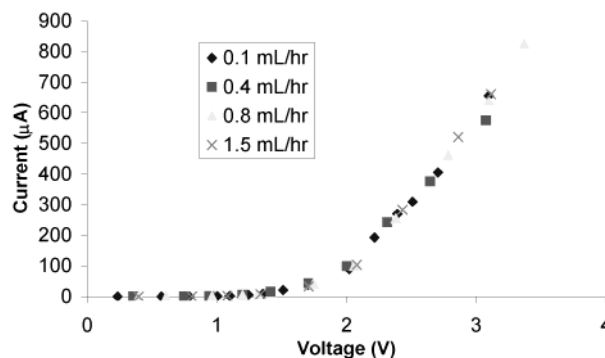


Figure 1. Measured current values as a function of flow rate using a platinum electrode system. The carrier was DI water.

ratio. At the very low ionic strengths used for the carrier solution (DI water), electrophoretic mobility tended to be constant across the particle size range,<sup>17</sup> which served to simplify comparisons between particles. Generally a value of  $-1.75 \times 10^{-4} \text{ cm}^2 \text{ V}^{-1} \text{ s}^{-1}$  was used as the mobility. Measurements of effective field were made with respect to particle size, flow rate, and applied voltage.

Plate height measurements have been made for general FFF systems, but little data regarding plate heights in EFFF systems have been reported. Plate heights in this work will be measured using 0.1- $\mu\text{L}$  acetone samples and standard chromatographic methods.<sup>23</sup>

Verification and testing of the basic retention equations were performed using two series of tests. The first series used a constant particle size and flow rate while the applied voltage was varied by steps up to the maximum voltage allowed in the system. This series of tests was analyzed by comparing the retention parameter to the inverse of the applied voltage and the inverse of the measured current, which should generate a linear relationship.<sup>10</sup> The second series of tests used a constant applied field and flow rate but varied the size of the polystyrene particles. The comparison for this series involved the  $\ln d$  and the  $\ln \lambda$ , which has also been shown to be a linear relationship.<sup>10</sup> Information related to the steric transition point was collected from these data sets.

Most of the parameters measured previously were compared to published data and data from our laboratory regarding macroscale EFFF systems. Results were compared to determine whether the advantages and disadvantages from miniaturization claimed in the preceding paper of this series are correct and whether there are significant advantages from scaling EFFF systems into the microscale domain.

## RESULTS AND DISCUSSION

**Current–Voltage Characteristics.** The current–voltage relationship for a channel fabricated with platinum electrodes is shown in Figure 1. There are two distinct regions to the graph. At low voltages, the currents are relatively small and indicate a lack of sufficient field strength to perform adequate separations. At 1.5 V, the current rises quickly in an approximately linear fashion. This “turn-on” voltage is characteristic of electrode systems of this type. In EFFF systems, the turn-on voltage varies

(19) Gale, B. K.; Caldwell, K. D.; Frazier, A. B. *Proc. SPIE* **1998**, 3515, 230–242.  
(20) Gale, B. K.; Frazier, A. B. *Proc. SPIE* **1999**, 3877, 190–201.  
(21) Brett, C. M. A.; Brett, A. M. O. *Electrochemistry: Principles, Methods, and Applications*; Oxford University Press: Oxford, U.K., 1993.  
(22) Figliola, R. S.; Beasley, D. E. *Theory and Design for Mechanical Measurements*; John Wiley and Sons: New York, 1991.

(23) Said, A. S. *Theory and Mathematics of Chromatography*; Dr. Alfred Huethig Publishers: Heidelberg, Germany, 1981.

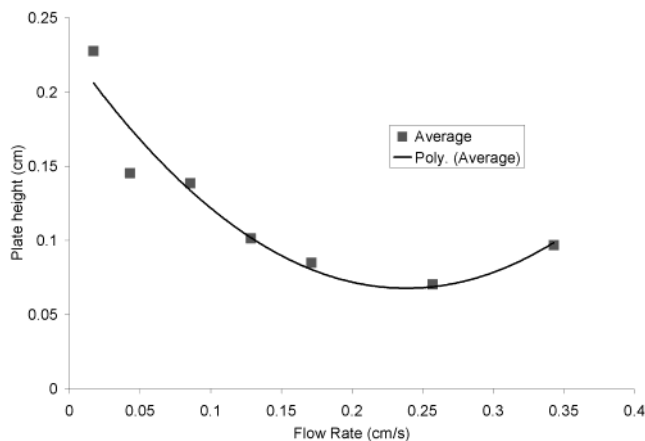


Figure 2. Plate heights for channel using off-chip detector for a series of flow rates showing rise in plate heights at low flow velocities due to diffusion in the connections and detector. Unretained acetone samples were used in these experiments.

somewhat with the overvoltage required for a given material—in this case platinum. Similar results have been reported by other groups using graphite electrodes, but with a lower required overvoltage.<sup>11</sup> Other data from our laboratory indicate that channels with gold electrodes have a somewhat higher turn-on voltage than either the platinum or graphite systems. Close examination of Figure 1 shows that the current–voltage relationship in microscale systems is unaffected by flow rate, in contrast to earlier reports with macroscale systems.<sup>11</sup> Also, current growth at low voltages (up to 1.5 V) is exponential, while at higher voltages the current growth slows somewhat, indicating a change in the limiting charge-transfer mechanism.

These data are useful in determining range of voltages that may be applied to produce a useful separation. Low voltages will not produce sufficient effective field for a separation, while voltages that are too high will generate bubbles from electrolysis (typically between 2.6 and 3.2 V). Thus, available currents range from  $\sim 1 \mu\text{A}$  to  $\sim 900 \mu\text{A}$ .

**Time Constants.** The measured time constant for a  $\mu$ -EFFF channel, 2 mm in breadth, 5.4 cm in length, and  $28 \mu\text{m}$  in height (average scale factor 0.11 compared to macroscale system), produced a time constant of less than 1 s. For channels with a larger area, time constants ranged from 1 to 4 s. These measurements compare favorably to the 40 s measured in a macroscale system.<sup>11</sup> These time constants fit well with the theoretical scaling effect for time constants predicted in the previous paper of this series.<sup>8</sup>

These results indicate a significant advantage to miniaturization in the area of system setup. For macroscale systems, the relaxation time at startup is  $\sim 200$  s, or  $5\tau$ . The relaxation time in  $\mu$ -EFFF systems would be no more than 20 s and could be as little as 4 s. The smaller time constants may allow for separation of particles using cyclic electric fields.<sup>24,25</sup>

**Plate Heights.** The earliest results of plate height measurements are presented in Figure 2. Examination of this figure indicates an unanticipated side effect of miniaturization: increasing plate heights at low flow rates. Diffusion is known to increase plate

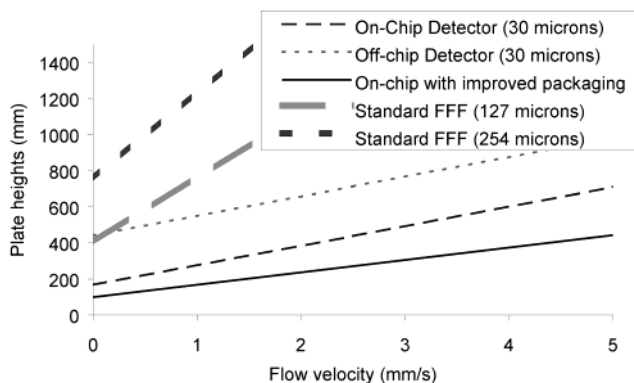


Figure 3. Comparison of measured plate heights for several EFFF systems. Acetone sample was used in all cases.

heights at low flow rates but was not expected to play a significant role until dimensions became much smaller. The increased plate heights seem to be related to diffusion and the mixing of the sample as it moves through fluid interconnects and flow channels with significant changes in cross-sectional area on its way to the off-column detector. Clearly the continued use of this detector with the microsystem would prove problematic.

Accordingly, the on-column detector was developed and the results of band-broadening calculations for the integrated  $\mu$ -EFFF system as well as several other FFF systems are shown in Figure 3. The results indicate that the premise that thinner channels produce smaller peak broadening is only true if the instrumental band broadening, indicated by the  $y$ -intercept on the graph, is small. Note the great improvements made in band broadening by improving the macro-to-micro interfaces and switching to an on-chip detector. The parabolic plate height characteristic of off-chip detection at low flow rates (Figure 2) is replaced with a linear characteristic over the same flow rate range. Other work in our laboratory indicates that continued improvements in this array may produce plate heights at the sub- $10\text{-}\mu\text{m}$  level if the packaging, detection, and injection systems are optimized.

**Retention.** Figure 4 demonstrates the linear relationship between  $\lambda$  (a nondimensional parameter relating the effect of the applied field and diffusion to the retention ratio,  $R$ ) and the inverse of current and is similar to results obtained using a macroscale system.<sup>10</sup> Since the current is directly related to the effective field in the channel, a logical extension can be made that the effective field also varies inversely with  $\lambda$ . The fact that the line through the data series nearly goes through zero validates the assumption that the current is a good measure of the effective field.

Another important retention relationship is that between the retention parameter,  $\lambda$ , and the particle diameter,  $d$ . This relationship forms the basis for the size selectivity parameter,  $S_d$ . For EFFF systems, the size selectivity is normally assumed to equal 1, but there is some question as to whether this assumption is valid. Earlier reports from macroscale data measured an  $S_d$  of  $\sim 0.67$ ,<sup>10,14</sup> while later systems were shown to have a  $S_d$  of  $\sim 1$ , as assumed.<sup>17</sup> Nevertheless, measurements in this area would be valuable and help to determine the efficiency of the system in separating particles based on size. Due to difficulties in maintaining constant separation parameters over time, data in this area can become smeared. These run-to-run variations can be eliminated by running multiple particle diameters in a single separation

(24) Giddings, J. C. *Anal. Chem.* **1986**, *58*, 2052–2056.

(25) Stevens, F. J. *J. Biochem. Biophys. Methods* **1990**, *20*, 275–292.

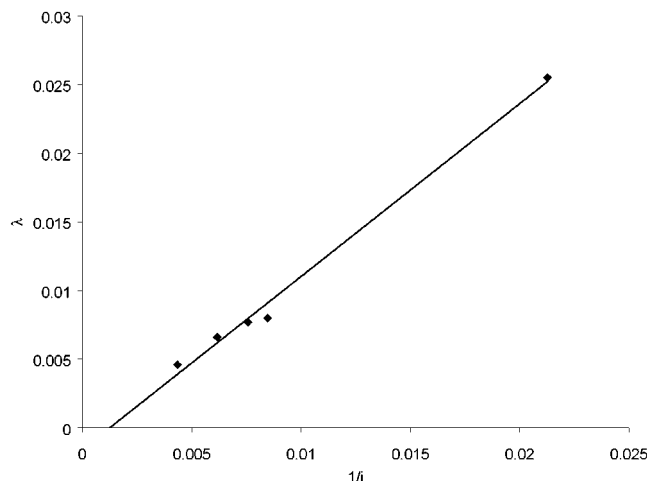


Figure 4. Retention parameter,  $\lambda$ , compared to the inverse of the measured current,  $i$ . The sample runs are performed using 94-nm PS particles in DI water with a flow rate of 0.3 mL/h in the system with platinum electrodes.

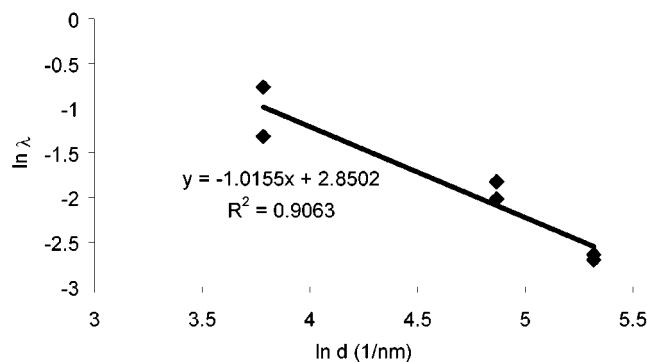


Figure 5. Natural logarithm of retention parameter,  $\ln \lambda$ , compared to the natural logarithm of particle diameter,  $\ln d$ . These results from two identical runs using 44-, 130-, and 204-nm particles in a DI water carrier. The three particle sizes give a measured selectivity parameter of 1.01.

as shown in Figure 5. This figure shows data from two identical runs that give a size selectivity of 1, showing that the microscale systems can generate separations close to the ideal. Practically, most of the separations do not show as high a size selectivity and early results in the system hovered around a size selectivity of 0.67, which was similar to the results published for the many macroscale systems.<sup>10,14</sup> Size selectivity in the macroscale systems was improved by adjusting sample injection methods and working at higher fields.<sup>16</sup> A similar protocol may be required to achieve consistently better results in the microscale systems.

**Stop Flow and Sample Equilibration Times.** In  $\mu$ -EFFF systems, it became apparent that there was little benefit from a stop flow period. Even small particles could be clearly retained without a stop flow period. Since the estimated stop flow times were typically only 1–2 s, the fact that the separations were not improved by using a stop flow period is not a surprise. Thus, for most experiments performed in the  $\mu$ -EFFF system, the stop flow time was eliminated.

**Separations.** Figure 6 shows a high-speed separation in a  $\mu$ -EFFF system with an on-chip detector. This separation demonstrates the ability of the system to separate polystyrene particles based on size. Under the same conditions, the time required for

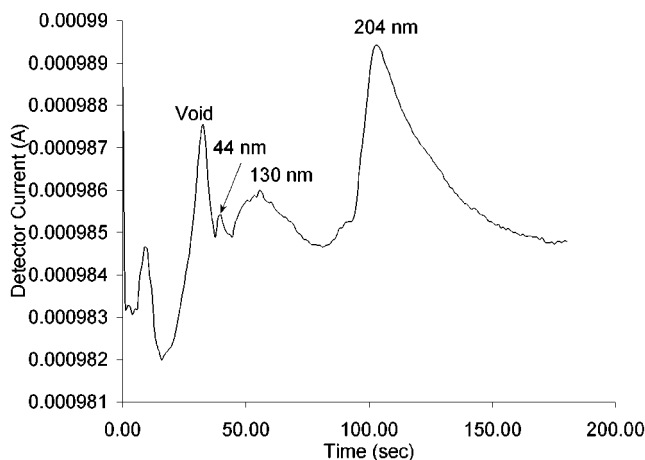


Figure 6. Separation of 44-, 130-, and 204-nm PS particles with on-chip conductivity detector. There is some fronting in the peaks due to the relatively high flow rate. Voltage was 1.6 V, flow rate was 0.3 mL/h, and current was 27  $\mu$ A. A 2-mm-wide platinum channel was used for this analysis. Carrier was DI water.

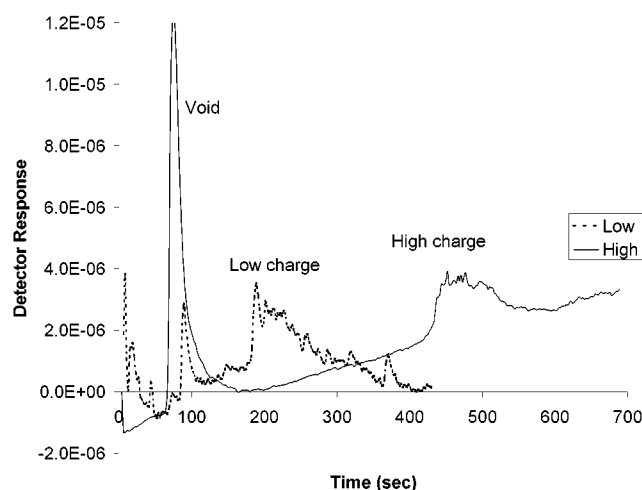


Figure 7. Fractograms of particles with the same diameter, but differing levels of carboxylation. The run labeled “low” had a lower density of COOH groups on the surface (67  $\mu$ equiv/g) and a correspondingly lower surface charge, so the particles eluted sooner than did those with a greater surface charge, labeled “high” (510  $\mu$ equiv/g). Carrier was DI water, voltage was 1.392 V, current was 10  $\mu$ A, and flow velocity was 1.48 mm/s.

a separation with similar resolution in a macroscale EFFF system would be  $\sim$ 2 h compared to the 2 min. While the resolution in these results is now only beginning to approach that seen in macroscale systems, the time required for those separations has been reduced. Part of the timesaving seen in this separation is due to the on-chip detector and the fact that there is no longer a need for sample transport off-chip. One concern with the detector used is the regular shifts in baseline seen here, which on occasion can make the analysis much more difficult.

EFFF also has the ability to separate particles by charge and not just size. Particles of identical diameter but differing surface charges were retained differentially in the  $\mu$ -EFFF system as shown in Figure 7. The particles were carboxylated polystyrene particles with nominal diameters of 160 nm. The only differences between the particles were the density of COOH groups on the particle surface, which gave the particles slightly different elec-

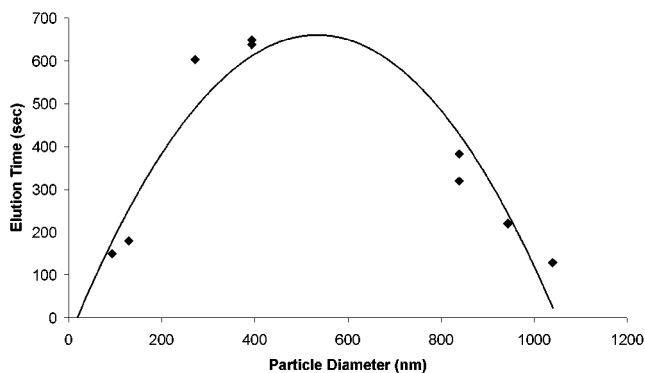


Figure 8. Steric transition point estimation for a platinum electrode system. Currents were kept at  $\sim 25 \mu\text{A}$  and flow rates at  $0.5 \text{ mL/h}$ .

trophoretic mobilities. The charge density for the particles labeled "high" was  $510 \mu\text{equiv/g}$  and  $67 \mu\text{equiv/g}$  for the particles labeled "low." The jagged peaks seen in Figure 7 occurred in several other runs and are thought to be artifacts in the detector, though they may in fact represent small bands in the separating particles themselves. Further analysis and characterization of this prototype detector will need to be performed to further answer this question.

**Steric Transition.** The steric transition point<sup>26</sup> was found for polystyrene particles using two different systems, with the results from one system shown in Figure 8. For the original gold electrode system, the steric transition point was found to be  $\sim 450 \text{ nm}$  for an applied voltage of  $2.0 \text{ V}$ , a current of  $\sim 145 \mu\text{A}$ , and a flow velocity of  $0.99 \text{ mm/s}$ . Using these values and the simple model for steric transition, the effective field can be roughly estimated at  $2.43 \text{ V/cm}$ . This value corresponds to an effective voltage that is  $0.34\%$  of the applied voltage. The results for the platinum system were slightly different, as is shown in Figure 8. The data for this system were collected using an applied voltage of  $1.275 \text{ V}$ , a current of  $\sim 25 \mu\text{A}$ , and a flow velocity of  $2.48 \text{ mm/s}$ . These data show a steric transition point of  $\sim 538 \text{ nm}$ , which gives a value for the effective field of  $1.89 \text{ V/cm}$ . This value is  $\sim 0.41\%$  of the applied voltage. Both figures indicate that the expected field strength is somewhat less than that obtained in macroscale systems. Wall repulsion effects are known to exist and complicate the simple steric transition model used in these calculations, possibly also complicating the interpretation of the results. These forces would become more important as the particles became smaller, since larger particles may not be as highly impacted by effects close to the surface. Other investigators have experienced similar results and have added the factor  $\gamma$  to the equation defining the steric transition point to account for these unexplained results.<sup>27</sup>

**Effective Field Measurements.** The most critical measurements concerning scaling in  $\mu\text{-EFFF}$  systems are the effective field measurements. If the effective field scales linearly, then most of the other scaling effects are expected to behave in the predicted manner. The effective field, as discussed previously for macroscale systems, is not as closely linked to the applied voltage as it is to the measured current, so difficulties can quickly arise in the analysis of scaling effects that are dependent on voltage. As with macroscale systems, though, the microscale system shows a linear

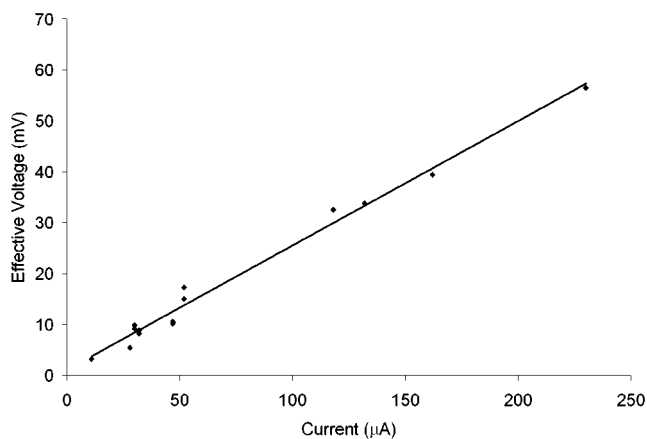


Figure 9. Current and effective field measurements in a  $\mu\text{-EFFF}$  with platinum electrodes. Standard particle diameters ranged between  $94$  and  $394 \text{ nm}$ .

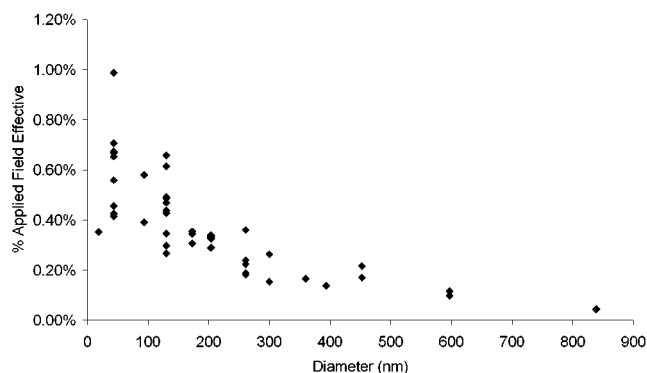


Figure 10. Percentage of the applied field that is effective compared to particle diameter. The low values for large particles are due to their separation in steric mode. All runs are performed in DI water. The scatter is related to the wide variety of run conditions used for the various experiments.

relationship between effective voltage and the measured current as shown in Figure 9. Thus, initial observations seem to indicate that the effective voltage and field will scale in a predictable manner.

Effective field strengths as high as  $3\%$  have been reported using water in macroscale systems,<sup>28</sup> though early systems rarely reported values over  $1\%$ .<sup>10</sup> Figure 10 shows the percent of the applied field that is calculated to be effective for a wide range of particle sizes in a microscale system. The fact that the effective field is dependent on the particle size may appear troublesome at first glance, especially to seasoned EFFF researchers, but the figure appears to demonstrate a microscale effect that may not have been noticed or considered before. A few superficial observations will be made first. The range of effective fields is quite similar to that obtained using the macroscale system in our laboratory. Second, the wide range in effective fields for a specific particle size is due to the use of a data from a wide range of separation conditions (as was shown in Figure 9). Figure 10 shows how the level of the effective field varies with particle diameter and is similar to the results reported in Figure 5.

With regard to the drop in effective field as the particle size increases, there appears to be a relatively straightforward answer.

(26) Giddings, J. C.; Myers, M. N. *Sep. Sci. Technol.* **1978**, *13*, 637–645.

(27) Myers, M. N.; Giddings, J. C. *Anal. Chem.* **1982**, *54*, 2284–2289.

(28) Tri, N.; Caldwell, K. D.; Beckett, R. *Anal. Chem.* **2000**, *72*, 1823–1829.

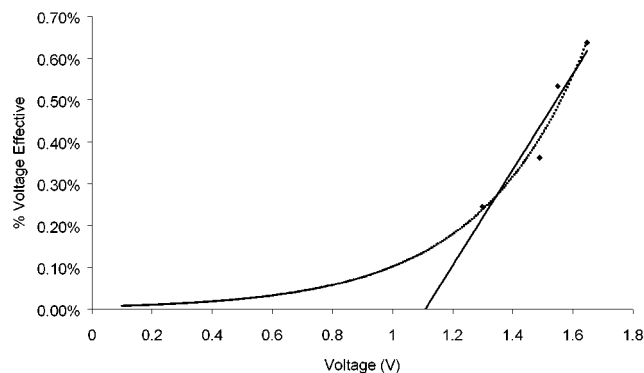


Figure 11. Percent effective field measurements as a function of voltage in a  $\mu$ -EFFF system with platinum electrodes.

For the microscale system, the calculated steric transition point lies somewhere between 300 and 500 nm for the typical operating conditions. Furthermore, the D/U layer thickness (i.e., the distance from the wall below which the majority of particles must reside to satisfy the theory) is much smaller in these microscale systems. While the layer thickness is often measured in micrometers for macroscale systems, the layer thickness in the microscale systems is typically in the same range as the steric transition point. For example, the calculated layer thickness in the platinum microscale channel used here for a typical voltage of 1.9 V (corresponding to 48  $\mu$ A) is 495 nm for 100-nm particles and 248 nm for 200-nm particles. For the macroscale channel, and the same retention value ( $R = 0.05$ ), the layer thickness for the 100-nm particles would be 18.7  $\mu$ m and for the 200-nm particles, 9.36  $\mu$ m. Thus, the ratio between particle size and layer thickness goes from 187 to 4.95 for the 100-nm particles and from 46.8 to 1.24 for the 200-nm particles. Consequently, in the microscale system, wall interactions and wall repulsion effects become much more significant, especially as the particles increase in size. Therefore, the trend seen in Figure 10 is showing the increasing influence of steric effects as the particle size increases. These results appear to explain the reduced size selectivity measured in many cases for microscale systems. These results demonstrate a limitation in smaller systems and may necessitate the use of even smaller particles and sample sizes to reduce sample-overloading effects.

The ratio between applied voltage and the effective voltage varies significantly depending on the materials and chemistries associated with the particular system and experiments. Accordingly, when a  $\mu$ -EFFF system with platinum electrodes was used, the effective field and the percentage of the applied field that was effective was greater than a system with gold electrodes. Figure 11 shows effective field data for the system fabricated using the platinum electrodes and separations using 94-nm particles. Figure 11 shows how the percentage of the applied field that was effective for retaining particles drops to nearly zero between 1.1 and 1.2 V. There are several things to note in this figure. First, the relationship between voltage and effective voltage is nearly linear above the point at which an effective voltage is generated. Second, as shown by the dashed curve in Figure 11, the data could fit an exponential curve that approximates the data presented earlier concerning the voltage–current characteristics of the channel in Figure 1.

Figure 9 and Figure 11, when viewed together point out some important considerations associated with effective fields in EFFF

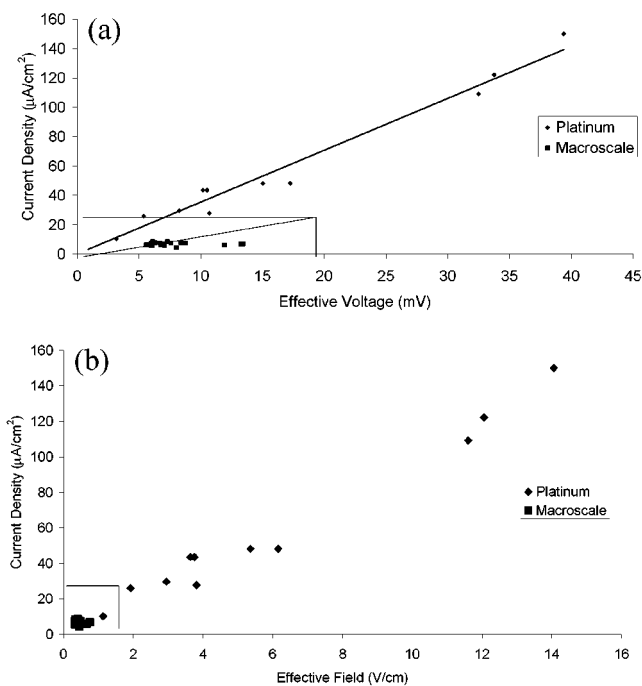


Figure 12. Comparing the electrical properties of a microscale system with platinum electrodes and the macroscale system. The boxes in both figures represent the limits of the macroscale system. (a) Comparison of effective voltage as a function of current density for the systems. The slopes of the two lines give an indication of the efficiency of the systems (i.e., power required for retention). (b) Functional relationship between effective field and current density.

channels. The first consideration is the material used for the electrodes. Comparing systems with differing electrode materials using the ratio between the measured effective field and the applied voltage can be misleading since it is clear that the electrochemical barrier at the carrier–electrode interface can vary significantly and cause geometrically identical channels to appear different (i.e., the channel with the lower electrochemical barrier would appear to produce relatively higher effective fields). The second characteristic that is important is that the current, applied voltage, and effective voltage all vary linearly with each other beyond the overvoltage associated with the electrode material. Thus, a reasonable suggestion for comparing separation abilities would be to subtract off the electrochemical barrier from the applied voltage and then perform the desired analysis or comparisons. The fact that the electrochemical barrier was not accounted for in earlier reports on microscale EFFF systems may explain why in many cases the intercept for these analyses was not zero.

Since current is directly related to the effective field, the macroscale and microscale systems can be compared by the retention that a specific current generates. Figure 12 shows how current density, which is used to account for channel size differences, varies with both effective voltage and effective field for both a microscale and the macroscale system. From Figure 12 it is clear that the macroscale system requires less current to generate the same effective fields or voltages seen in the microscale systems. Thus, the macroscale system is more efficient in terms of power required to produce retention. The cause of this difference is not readily apparent, but is most likely related to the material properties of the electrodes. Additionally, the

efficiency of the system decreases as the ionic strength of the carrier solution increases. All of the microscale measurements were made in DI water, while the macroscale measurements were made in buffered solution of up to 200  $\mu\text{M}$   $(\text{NH}_4)\text{CO}_3$ .

The boxes in both graphs of Figure 12 demonstrate the maximum current densities, effective fields, and effective voltages expected to be possible in the macroscale system. The limit, which is the onset of electrolysis of water, was found using previously published data from other researchers<sup>11</sup> and work performed in this laboratory using a macroscale system. These experiments clearly demonstrate that the microscale systems have a much greater capability than macroscale systems and a greater range of operation, while the same retention mechanism is still utilized since all the data points fall along a straight line. Also, Figure 12b clearly shows that the effective field in the microscale system can be 7–8 times higher than for the macroscale system, which is slightly better than that predicted by scaling alone (a ratio of 6.4 is expected). While this improvement is promising, it is not clear why there is a higher possible effective voltage for the microscale systems. The effective field is expected to increase due to the reduction in wall separation distance, but the effective voltage would be expected to remain constant. Three immediate possibilities present themselves. The first possibility is material dependent. The resistance across the interface for the platinum electrodes may be lower than for the graphite electrodes once the electrochemical barrier is reached, allowing a much higher current and the corresponding effective voltage and effective field. A second contributor is the carrier ionic strength, which was not (or unlikely to be) identical in the two systems since the obtained data were compared to data in the literature.<sup>11</sup> Ionic strength affects the slope of the lines in Figure 12a, so contamination either prior to the channel or in the channel could cause a change in the carrier resistance. The third possibility and the one most likely to have a direct impact, is that the microscale system was tested using smaller particles than was the macroscale system. As was shown in Figure 10, small particles appear to be separated more efficiently, whether that is because of steric effects, wall repulsion effects, or other nonlinear effects. The smaller particles used in the microscale system would therefore allow a higher effective voltage or field to be calculated for the microscale system. Thus, the difference between the two systems may be somewhat exaggerated and the total improvement may be closer to that predicted by scaling. Nevertheless, the improvement in effective fields is significant and consistent with the theory presented in the previous paper in this series.<sup>8</sup> Thus, it appears that concern over scaling of the electric fields during miniaturization of the EFFF channel is reduced.

**Other Scaling Advantages.** Several additional advantages derived from miniaturization are not directly related to the mechanism of separation in the EFFF channel but are outgrowths of the reduced size of the system. For example, the injected sample size was typically 0.1  $\mu\text{L}$  and never over 0.3  $\mu\text{L}$ , which volume was occasionally required to increase the detectability of the sample. This compares to typical macroscale sample injections of 5–10  $\mu\text{L}$ . Significantly, the injected sample should be 10 times smaller than the 0.1  $\mu\text{L}$  used in this work based on scaling alone. Further sample size reductions were limited, though by detection and sample injection difficulties. A related advantage

Table 1. Comparison of Predicted Scale Factors to Measured Scale Factors

parameter	predicted scale factor	actual scale factor	consistent?
retention ratio ( $R$ )	1	$\sim 1$	yes
analysis time	$s$	$s$ or better	yes
plate height ( $H$ )	$s^2$	$s$ or less	no
resolution ( $R_s$ )	$1/\sqrt{s}$	increase	yes
steric transition ( $d_t$ )	$1/\sqrt{s}$	decrease	yes
equilibration time ( $\tau_e$ )	$s^2$	decrease	yes
field time constant ( $\tau$ )	$s$	$\sim s$	yes
required sample size	$s^3$	$\sim s^2$	yes
solvent consumption	$s^3$	$s^3$	yes
instrument size	$s$	$s^3$	yes
separable particle size	$s$	$s$	yes

involves carrier consumption, which was reduced by a factor of nearly 1000.

Finally, the instrument size has been reduced significantly. The macroscale channel used in this work for comparison (not including any enabling components) is about 80 cm long, 10 cm high, and 10 cm wide and weighs  $\sim 25$  lb (10 kg). While more recent advances in macroscale technology have reduced those dimensions somewhat, they are still significantly larger than the microscale channel, which is similar in size to a stick of chewing gum. The microscale system is about 7.5 cm long, 2 cm wide, 1.5 mm in height and weighs  $\sim 50$  g. Clearly the microscale channel is reaching a point where it takes up almost negligible space in the laboratory. Unfortunately, the associated instrumentation (power supplies, pumps, data acquisition equipment) has still not been completely miniaturized and can be quite bulky.

## CONCLUSION

Examination of the relevant data clearly indicates that the miniaturized EFFF system operates according to the theory for miniaturized systems and therefore can claim all of the advantages associated with that theory. A summary of the important scaling parameters and how they have been shown to vary experimentally is presented in Table 1.

A few specific results are worth noting from Table 1. Overall plate heights did not improve as much as predicted by scaling, but that is mostly due to instrumental contributions to the plate height such as sample injection method, and interfaces to the microchannel. Diffusion at very low flow rates may have also been a contributor. The required sample size for use in the  $\mu$ -EFFF channel dropped significantly, but detectability limited the minimum injection volume. Most importantly, the electric field strength scaled according to the theory as well. The one limitation to the scaling theory appeared when relatively large particles were used in the system and steric effects began to affect the separations. Nevertheless, the abilities and performance of the  $\mu$ -EFFF system showed improvements over the characteristics of macroscale systems.

Received for review September 13, 2001. Accepted December 7, 2001.

AC015623P